AeroEnergy Consulting
7 Strathridge Gardens SW, Calgary, AB, Canada T3H 3S1

Proof of Concept Simulations

September 5th 2019

Project: Vortex Vacuum Chamber – Proof of Concept
Client: Infinidium Corp. (Att. Mr. Paul Gill)
Consultants: Dr. Arman Hemmati $_{EIT}$

EXECUTIVE SUMMARY

The CAD model of the original- and modified-design of the Vortex Vacuum Chamber concept was completed including the GPUs, battery housing unit and other required components of the chamber. A simplified geometry was used to simulate the proof-of-concept air natural convection inside the Vortex Vacuum Chamber in steady and unsteady states. The chamber drive the flow solely based on buoyancy effects, which is based on temperature differences between the inlet and the outlet. The results provided evidence that the modified design of the chamber can maintain a constant temperature of 89 degree Celsius (maximum operating temperature of GPUs) with an ambient temperature of 20 degree Celsius from the inlet. The constant temperature at the walls (89 degree Celsius) is the critical operating state, which proves the reliability of design in maintaining a sufficiently low temperature inside the chamber at all other states of operation. The air inside the chamber cooled down to the ambient temperature within 0.3 inches (<0.5% of chamber diameter) from the wall. This was consistent across the entire height of the chamber. The regions at the bottom of the chamber (imprisoned between the battery housing unit and GPUs at the wall) experience the highest temperatures.

It was determined that placement of converging-diverging nozzles at the outlet of the chamber obstructs the flow of air since nozzles operate in a pressurized system. However, natural convection of air, which is the basis of Vortex Vacuum Chamber, is a pressure-temperature driven process that cannot provide the sufficiently high pressure required for the flow in the nozzle. If the nozzle was placed at the outlet, a fan must be used to force the airflow through the chamber and pressurize the system.

INTRODUCTION

Design and analysis of a cooling chamber, incorporating natural ventilation through buoyancy-driven airflow, was investigated to provide the proof-of-concept for the proposed Vortex Vacuum Chamber. The objective of this project is to analyse the airflow inside the chamber and facilitate natural convection of residual heat emitted from the GPUs and battery stack. Natural ventilation properties are approximated using Boussinesq approximation to solve the fluid flow equations. Natural ventilation is a passive cooling strategy that utilizes temperature differences to drive the flow of air. The buoyancy effect drives the flow using the differences in density and the resultant weight of the fluid.

CAD Models

Two Computer Assisted Design (CAD) models were developed for the original design and modified (optimized) design of the chamber. These models are shown below, and their respective engineering plans have been shared with the client through email on July 12th as per the project deliverables. The engineering drawing of the modified design of the chamber has been included in the appendices.

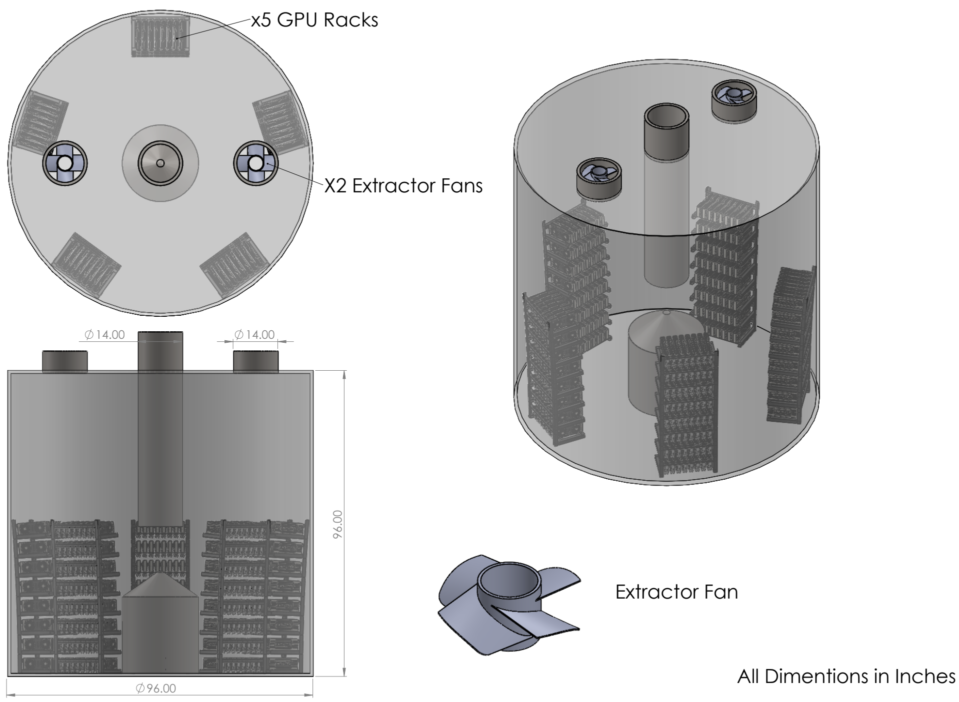

Figure 1: CAD model of the original design of the Vortex Vacuum Chamber

Preliminary simulations revealed that nozzle shape of the air-outlet on top of the chamber physically obstruct the flow of air into the chamber. The nozzle flow is a pressure-driven process and requires a pressurized system. However, natural convection is a pressure-temperature driven phenomenon, which cannot provide the necessary pressure difference to allow for airflow through the chamber. In order to place the nozzle on top of the chamber, we need to use forced convection of air via a fan. Thus, we decided, and notified the client on July 17 2019, that this design feature is not practical. Thus, the nozzle will not be considered in simulating the proof-of-concept. The outlet nozzle is replaced with a single cross-section short pipe as shown in Figure 3.

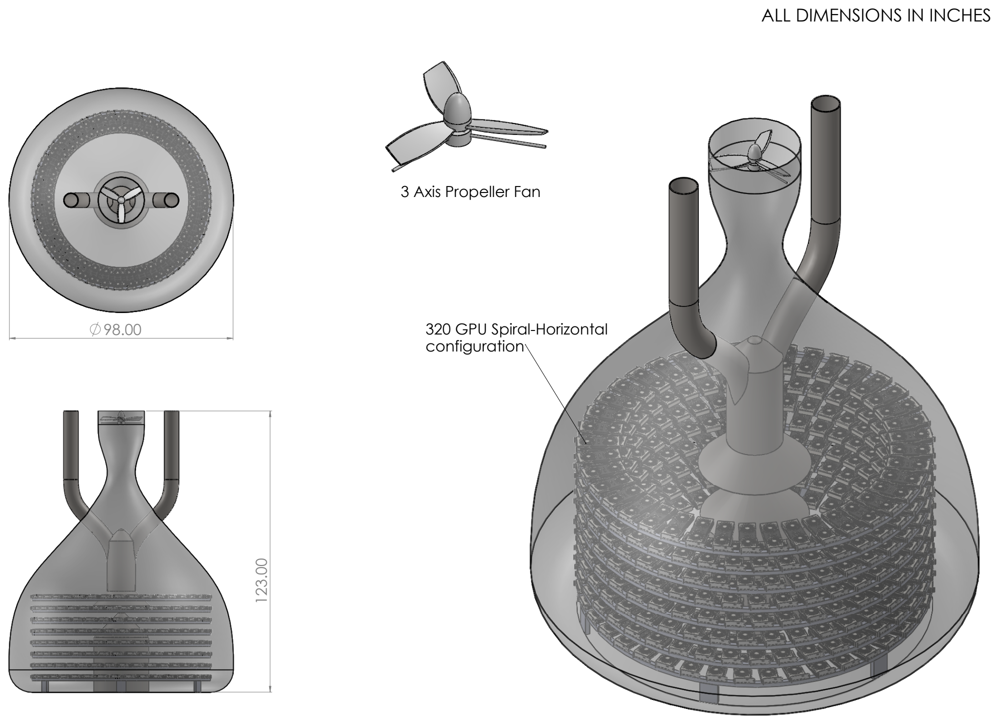

Figure 2: CAD model of the modified design of the Vortex Vacuum Chamber

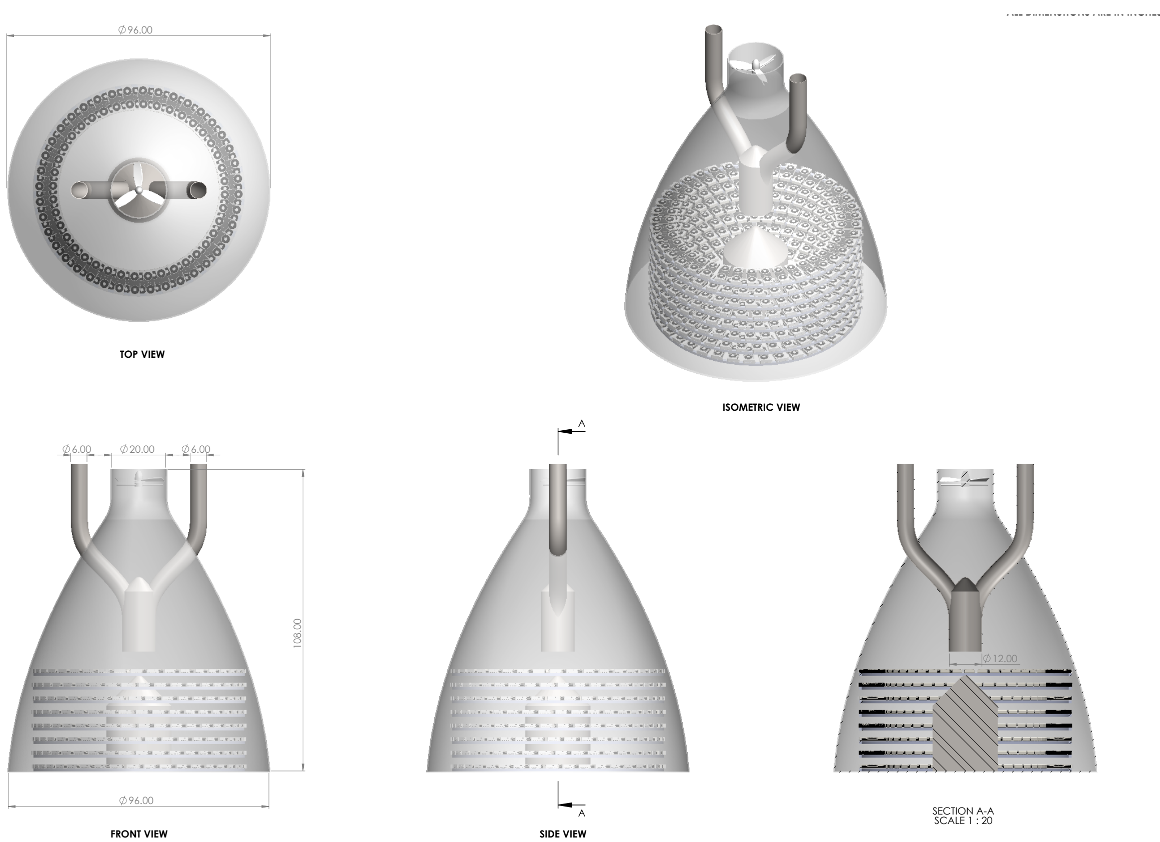

Figure 3: CAD model of the practical modified design of the Vortex Vacuum Chamber. All dimensions are in inches.

PHONE
+1-403-5614723

EMAIL
info@aeroenergyc.com

WEB
www.aeroenergyc.com

SIMULATION GEOMETRY

The geometry that was designed for simulations reflected a simplified version of the actual design to enable effective but still accurate observation of the proof-of-concept. Initially, a two-dimensional chamber was simulated in steady state using RANS k-ε model in OpenFOAM. The design of cooling chamber consists of a looped battery stack in the centre of the chamber (24-inch height by 24-inch width), and the chamber had a standard office space size (96-inch width by 108-inch height). These dimensions are selected to allow accessibility into the chamber as per the clients' request. The chamber will incorporate approximately 300 GPUs. For simplification, inlet conditions are enforced inside the chamber instead of simulating the flow through the two inlet pipes that form the inlet in the actual design. The air temperature at the inlet is assumed to be that of the ambient air, and the hydrostatic pressure difference is incorporated in the inlet boundary condition for pressure. Figure 4 shows a schematic of the simulated chamber. The design criteria were set to be constant temperature at the chamber walls, and the flow was simulated to determine the temperature distribution in the chamber.

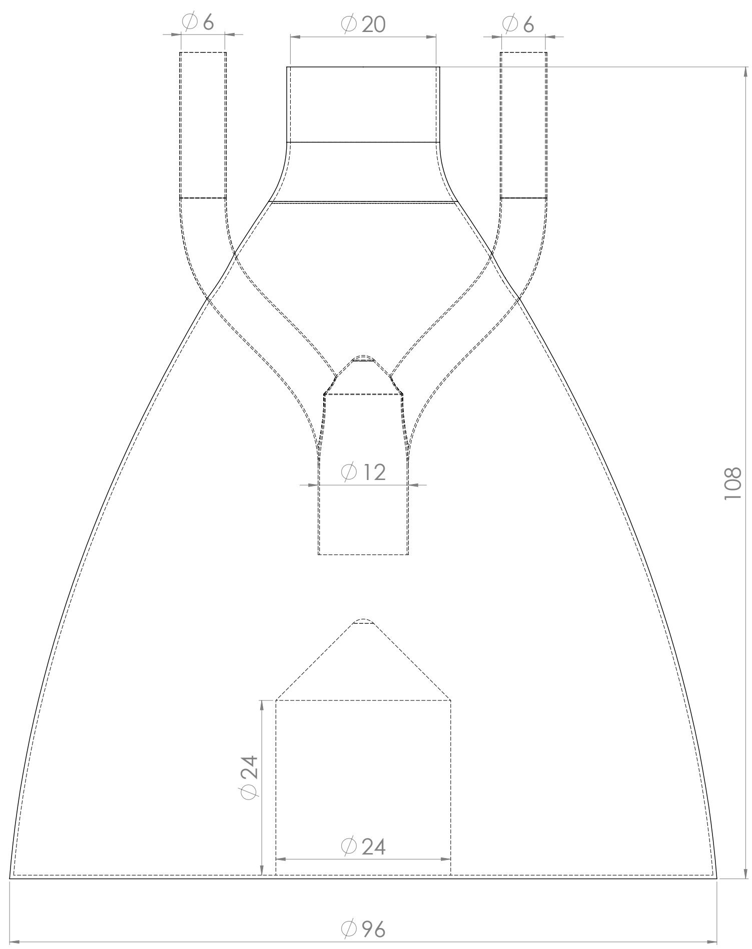

Figure 4: Schematics of the simplified geometry of the Vortex Vacuum Chamber for proof-of-concept simulations

FLOW PROPERTIES

The flow is assumed to be steady state and incompressible with constant density in continuity and momentum equations. The body forces were due to density variation caused by temperature differences. Here, k- ε turbulence model is selected because the flow is pressure-temperature driven and hence a laminar flow cannot be maintained.

Table 1: Flow Properties

Property	Value
Fluid	Air
Density (ρ) at 25 °C	1.185 kg/m^3
Viscosity (ν) at 25 °C	9.89 X 10^{-6} m^2/s
Coefficient of Thermal Expansion	3.36 X 10^{-3} /K
Turbulent Kinetic Energy (k)	0.0326 m^2/s^2
Epsilon	3.13 X 10^{-3}

BOUNDARY CONDITIONS

The boundary conditions assigned for this simulation are provided in Table 2. These conditions best describe the natural convection of air to cool a heated chamber wall, representing GPUs operating at their maximum temperature. This setup enables examining capabilities of the chamber concept in maintaining low air temperature inside the chamber if the walls are constantly at a high temperature (constituting constant heat flux by GPUs).

Table 2: Boundary conditions for the simulations

Boundary	Condition
Inlet	Fixed value velocity (0, -0.609, 0), approximated from pressure driven flow and opening-type inlet boundary.
Outlet	Fixed value pressure, outlet direction only.
Heated Walls	Fixed Temperature of 89 °C (362.15 K).
Battery Walls	Fixed Temperature of 50 °C (323.15 K).
Walls	Adiabatic walls, no slip.
Front	Symmetry
Back	Symmetry

NUMERICAL SETUP

All simulations are completed using OpenFOAM, an open-source continuum mechanics/Computational fluid dynamics tool. Steady-state simulations are completed using “BuoyantBossinesqSimpleFoam” solver, which is a steady-state solver for buoyant and turbulent flows of incompressible fluid. ”BuoyantBossinesqPimpleFoam” solver is used for transient simulation. The table below lists all the numerical schemes used in the simulations.

Table 3: Numerical Schemes and setup

Parameter	Description
Time Scheme	Steady State
Gradient Scheme	Gauss Linear
Divergence Scheme	• Bounded gauss linear upwind scheme for Velocity and Temperature • Bounded gauss upwind scheme for k-epsilon.
Laplacian Scheme	Gauss linear orthogonal
Interpolation Scheme	Linear
Surface Normal Gradient Scheme	Orthogonal

MESHING AND MESH-INDEPENDENCE

A good quality mesh is essential for obtaining accurate results in CFD Analysis. Also, a structured tetrahedral mesh results in better convergence as well as better results. Thus, an inhomogeneous tetrahedral grid was used for the simulations. Three successive meshes are analysed, each with gradual refinement. Figure 5 show the spatial mesh created for these simulations. Table 4 states the details of these cases.

Table 4 : Mesh details

Mesh	Number of Grid points
Mesh 1	73372
Mesh 2	279708
Mesh 3	1125996

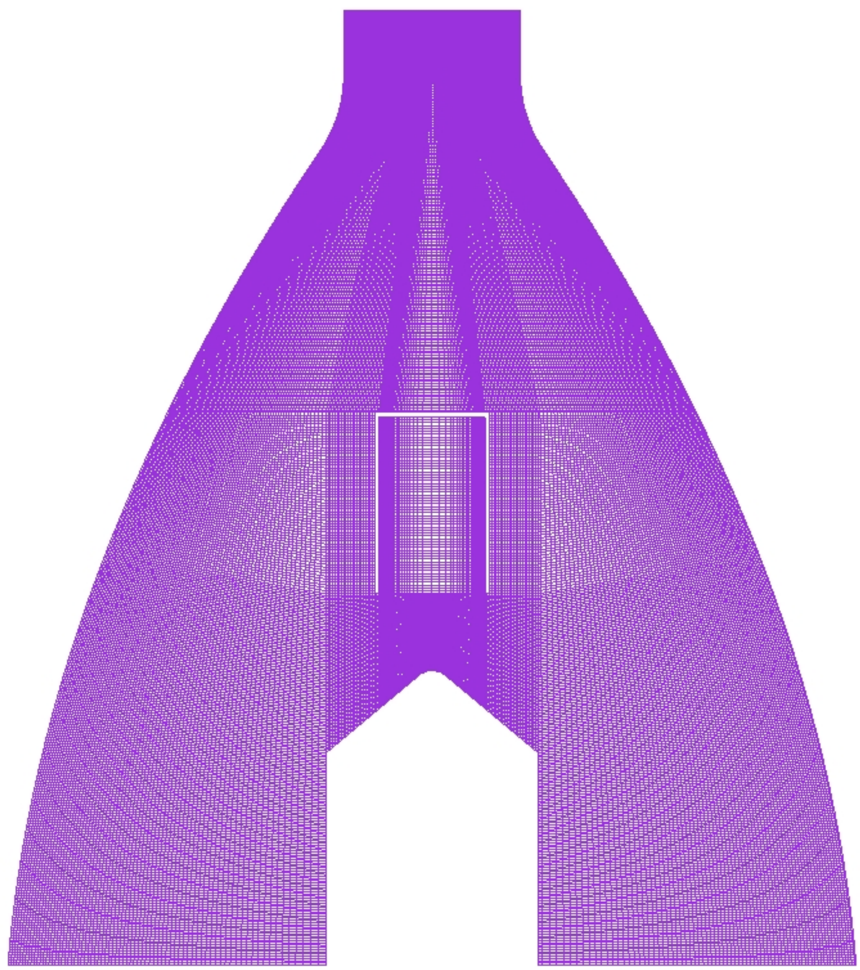

Figure 5: Schematics of the mesh for the Vortex Vacuum Chamber for proof-of-concept simulations

The boundary layers are refined to enable accurate simulation of the flow field and velocity gradients. This is shown in Figure 6, where the areas at the walls (including the chamber walls and those of the inlet) are refined. The growth rate is maintained at 1.03.

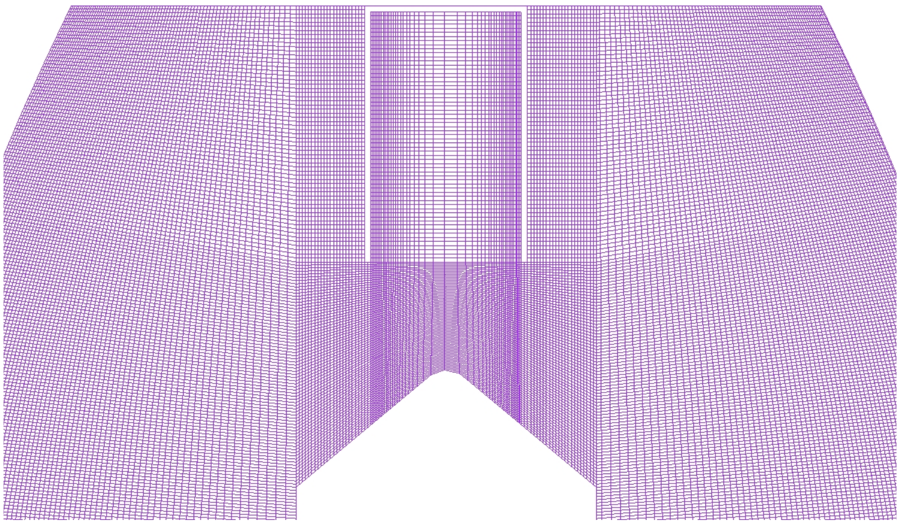

Figure 6: Schematics of the mesh refinement in the boundary layer near the walls

Mesh-independence study is conducted by probing temperature values of highest converged mesh at five critical locations in the chamber. These critical locations are selected based on flow conditions inside the chamber as well as locations of GPUs and battery pack. Temperature values are tracked at these locations with three successively refined meshes. Mesh independence is achieved when the relative change in temperature values between meshes are smaller than 10%. Figure 7 shows the five probe locations selected for this validation study.

The details of mesh independence study are presented for three case studies of Mesh 1, Mesh 2 and Mesh 3.

Table 5: Mesh independence results for probe locations 1, 2 and 3

Case Number	Number of Nodes	Probe 1	% Change	Probe 2	% Change	Probe 3	% Change
Mesh 1	73372	300.371	-	302.799	-	300.19	-
Mesh 2	279708	300.85	0.15946946	303.699	0.29722687	300.505	0.10493354
Mesh 3	1125996	301.703	0.28353	305.933	0.73559676	301.836	0.44292108

Table 6: Mesh independence results for probe locations 4 and 5

Case Number	Number of Nodes	Probe 1	% Change	Probe 2	% Change
Mesh 1	73372	304.275	-	301.326	-
Mesh 2	279708	305.162	0.29151261	301.828	0.16659697
Mesh 3	1125996	305.383	0.07242055	302.919	0.36146415

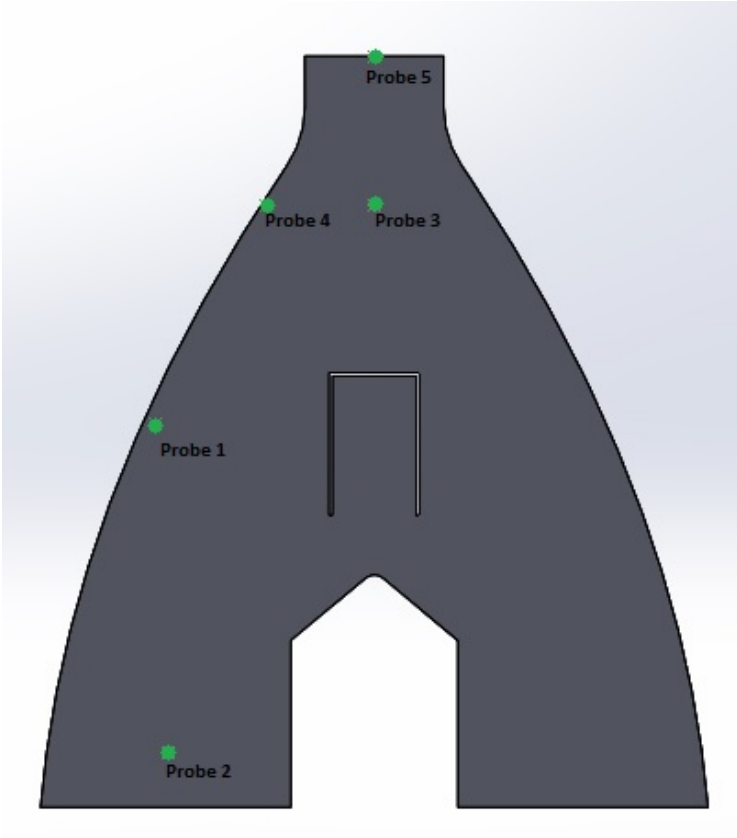

Figure 7: Probe locations for mesh-independence study

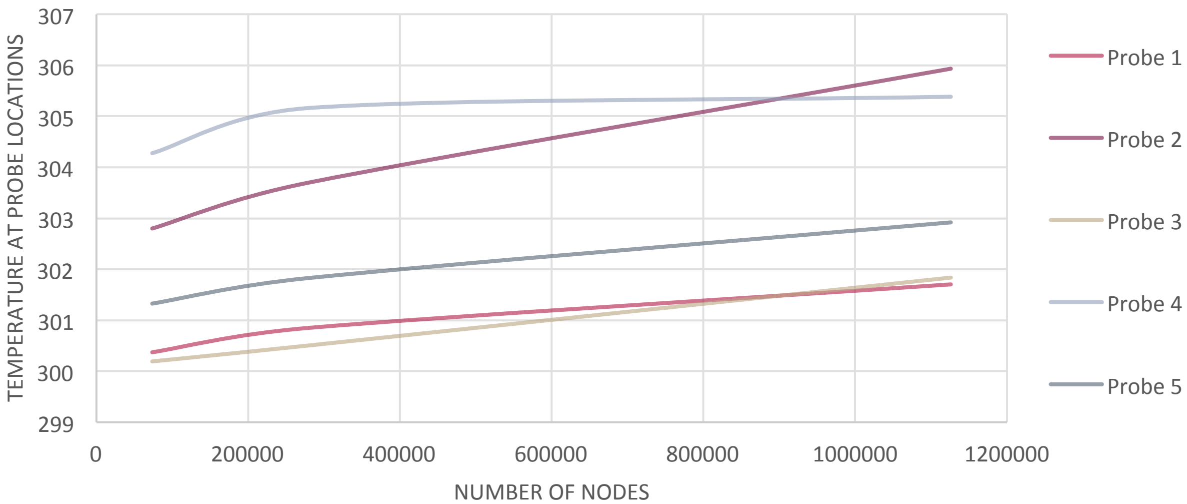

Figure 8: Mesh-independent analysis

The mesh- independent results are presented in Figure 8. These results show that the simulations have reached asymptotic range, in which the changes are small with mesh refinement after Mesh 2. Therefore, the numerical setup and mesh refinement of Mesh 2 is used for simulating the natural convection of air in the vacuum chamber.

RESULTS AND DISCUSSIONS

The contours of flow velocity, temperature and pressure are visualised to analyze the design. Contour plots of these quantities provide an estimation of cooling effects within the chamber. They are also helpful in visualizing the air flow inside the domain for facilitating the design. Figure 9 shows the contour plot for pressure distribution within the chamber. This plot agrees with pressure distribution created due to buoyancy-driven flows, which rely on pressure difference between inlet and outlet openings. Here it is noted that with increase in height of the chamber, the pressure normalises to ambient air pressure.

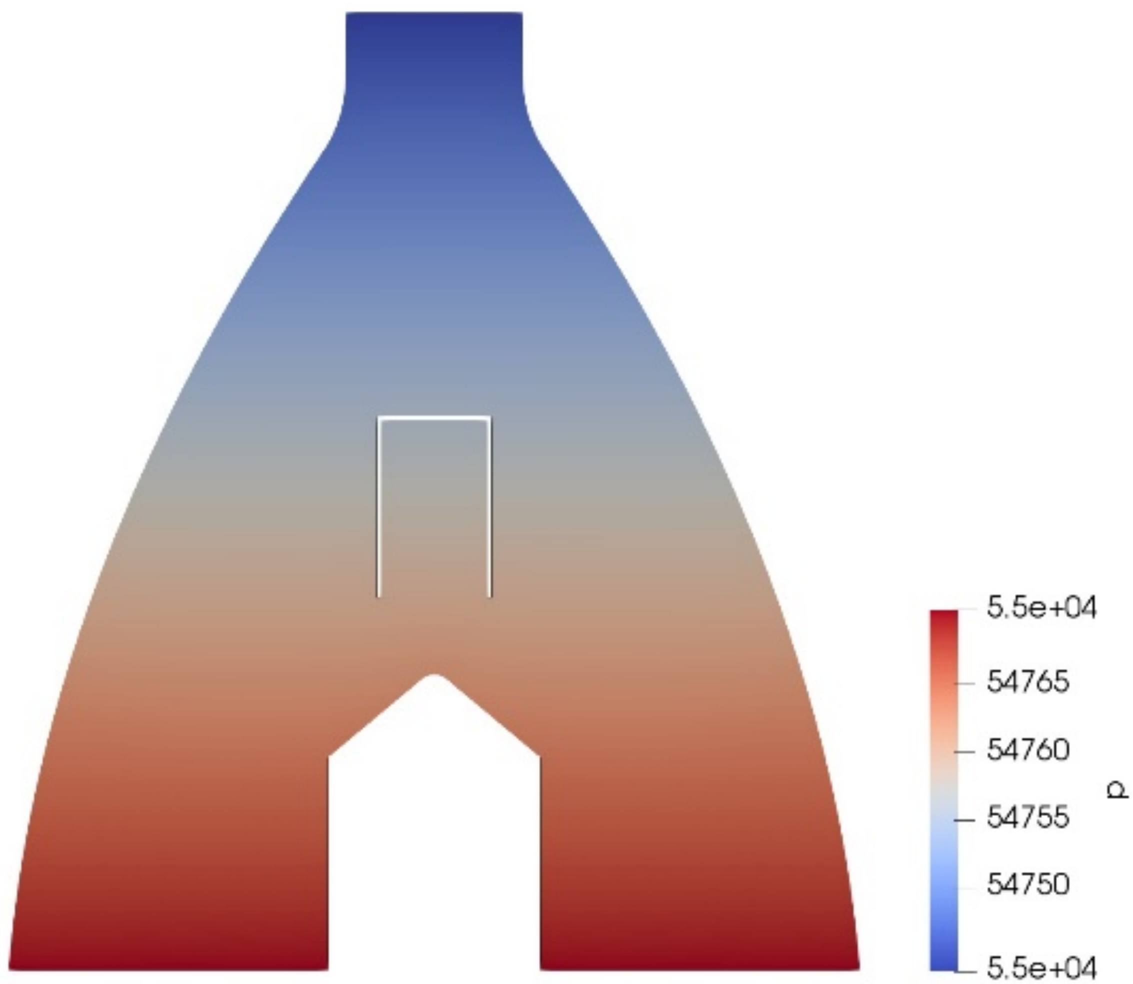

Figure 9: Pressure contour inside the chamber at operational temperature difference of 69 degrees Celsius.

Figure 10 shows the velocity contours inside the chamber. Velocity is approximated by the pressure difference between the inlet and outlet openings. As the cool air enters the chamber, the dome on top of the battery stack acts as a flow deflector to accelerate and distribute the flow. Air diverts towards the outlet and due to converging shape of the chamber, it again accelerates near the wall towards the outlet. The flow carries the residual heat generated from GPUs and battery stack, thus cooling the chamber by natural ventilation.

Figure 11 shows Temperature contours inside the domain. These plots show the cooling effects inside the chamber at steady state. Natural ventilation efficiently cools the chamber to an average temperature of 26 °C (300 K) within 0.3 inches from the wall (less than 0.5% of the chamber diameter). The space between the battery stack and lower wall of the domain show a slightly higher temperature (up to 23 degree C) due to heat generated from both battery stack and GPUs.

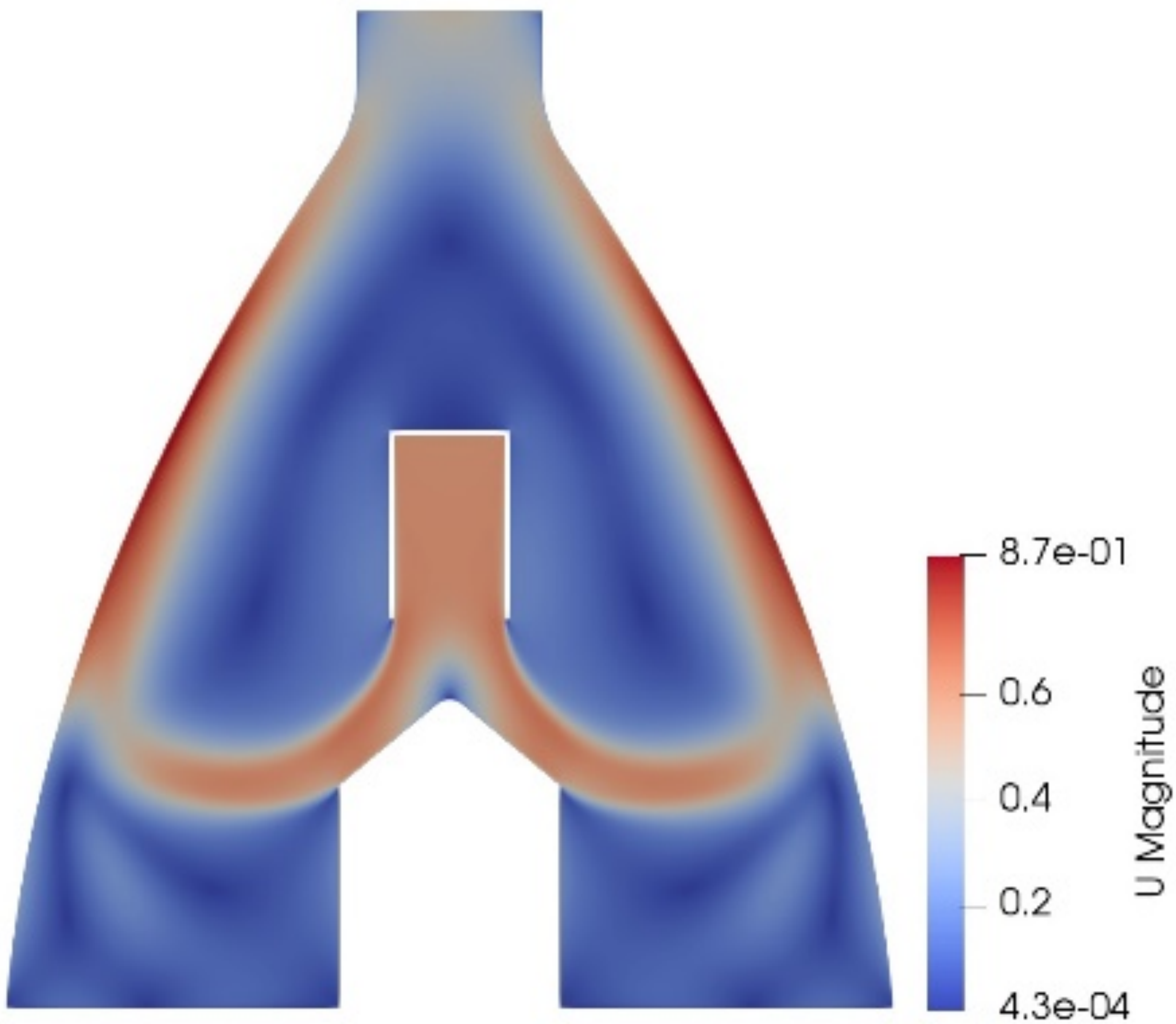

Figure 10: Velocity contour inside the chamber at operational temperature difference of 69 degrees Celsius

The cooling effect can be observed from the temperature distribution at different locations in the chamber, from wall towards the inside of the domain. Figure 12 lists lines over which temperature differences are plotted. These plots will show temperature distribution over a set of arcs from walls towards the center of the chamber.

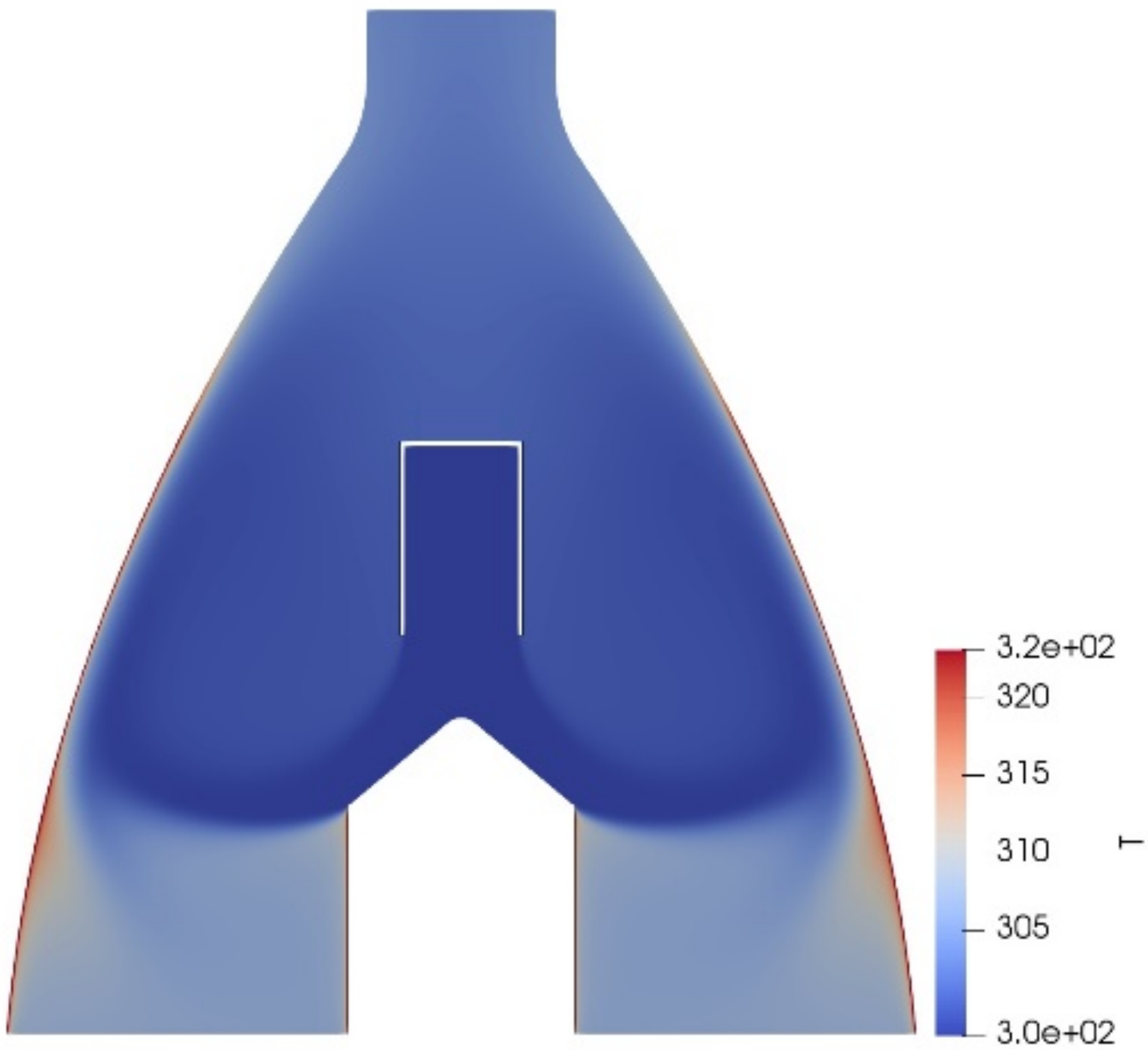

Figure 11: Contour of temperature inside the chamber scaled between 25°C and 50°C

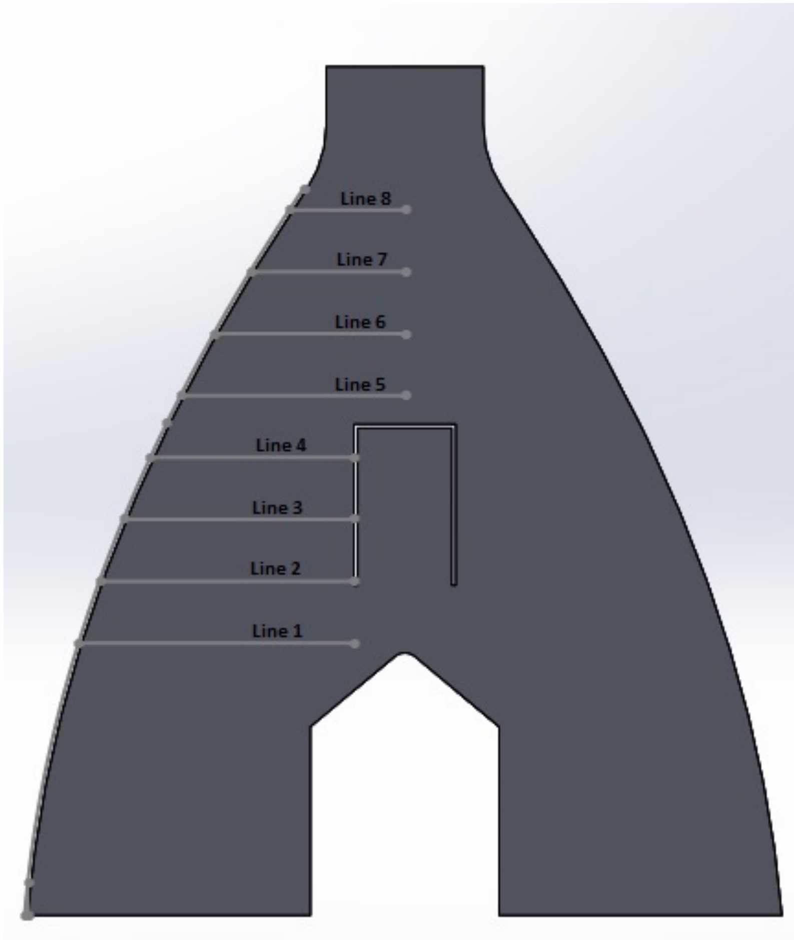

Figure 12: Location of temperature distributions inside the chamber.

The trend of temperature variation in different locations within the domain is shown in Figure 13. It is observed that temperature drops with distance from the wall towards the center of the chamber quickly within 0.3 inches. Going upwards towards the outlet, a higher temperature spectrum is observed. This shows that hot air is carried upwards towards the outlet, hence the higher temperature in that region. The temperature gradient within 0-0.3 inch from the wall corresponds to the boundary layer at the wall and their impact on the overall flow is insignificant.

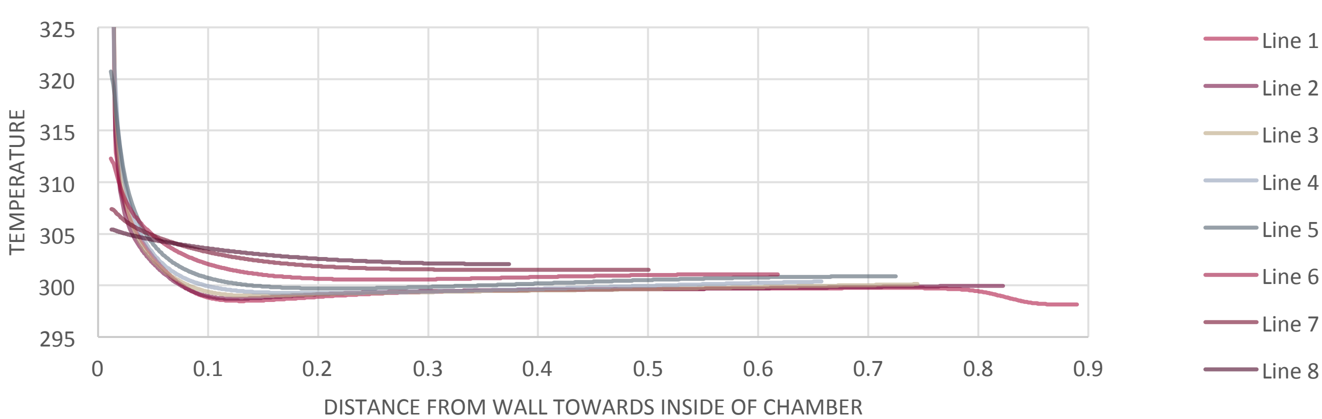

Figure 13: Temperature distribution at different locations in the chamber.

UNSTEADY SIMULATIONS

Based on the good results on Mesh 2, the unsteady flow is simulated over the period of stabilization until steady state is achieved for the air temperature inside the chamber. The animation of the flow is provided as a supplementary document to the client along with this report. Despite small fluctuations in the initial stages of the flow development, the final solution is identical to the steady state solution provided in this report.

OPTIMUM DESIGN OF CHAMBER

The results identify the optimum design of the chamber to have the battery unit placed in the floor. The inlet airflow also includes a distributor that directs the airflow into the bottom corners. The design is shown in Figure 14, and the engineering design of the optimum design is included in Appendix.

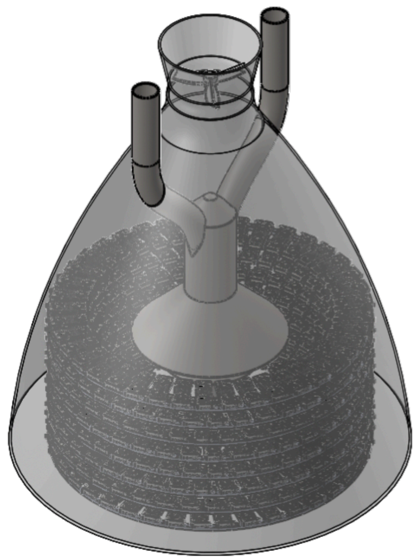

Figure 14: CAD model of the practical modified design of the Vortex Vacuum Chamber. All dimensions are in inches.

CONCLUSIONS

The results presented here show that the concept of vacuum vortex chamber is validated. It facilitates the flow of air by natural convection due to the temperature differences between the inlet and outlet resulting from the constant temperature at the walls of the chamber. Thus, the modified conceptual design of the chamber without a nozzle placed at the outlet can maintain room temperature while the wall temperature is kept constant at the maximum operating temperature of GPUs. This design criterion proves the concept of the Vacuum Vortex Chamber for its set purpose.

APPENDIX A: Original Concept Design of Vacuum Chamber

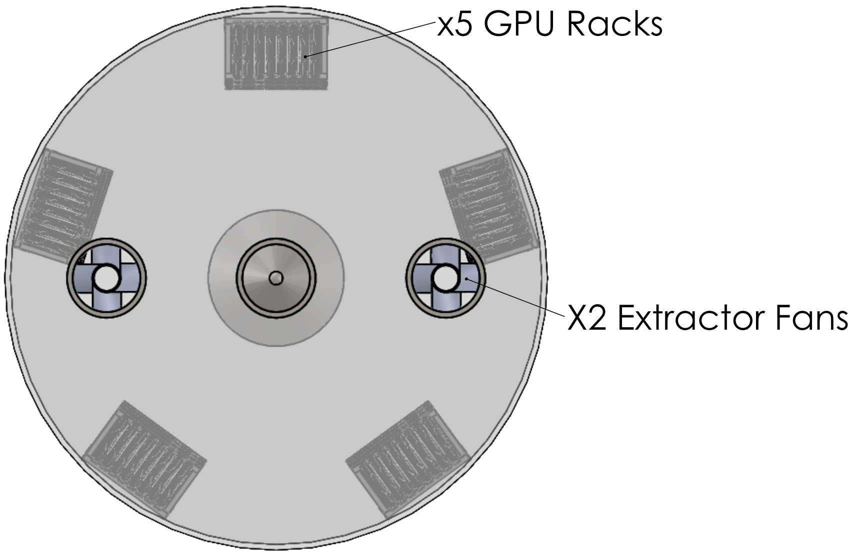

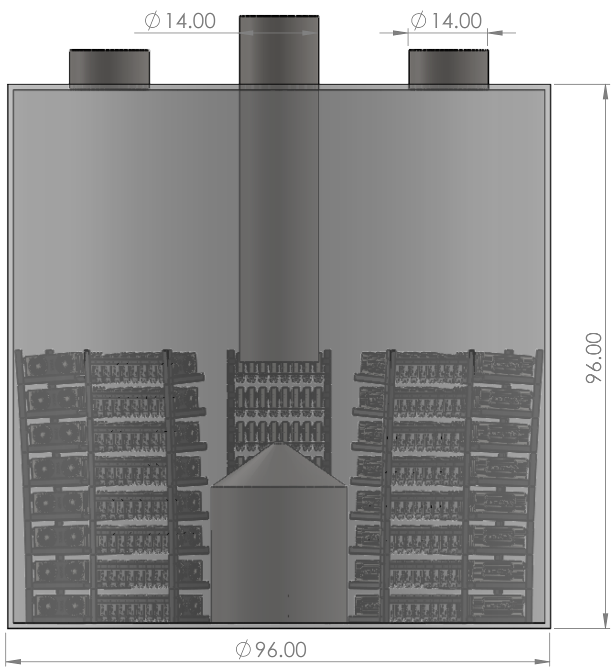

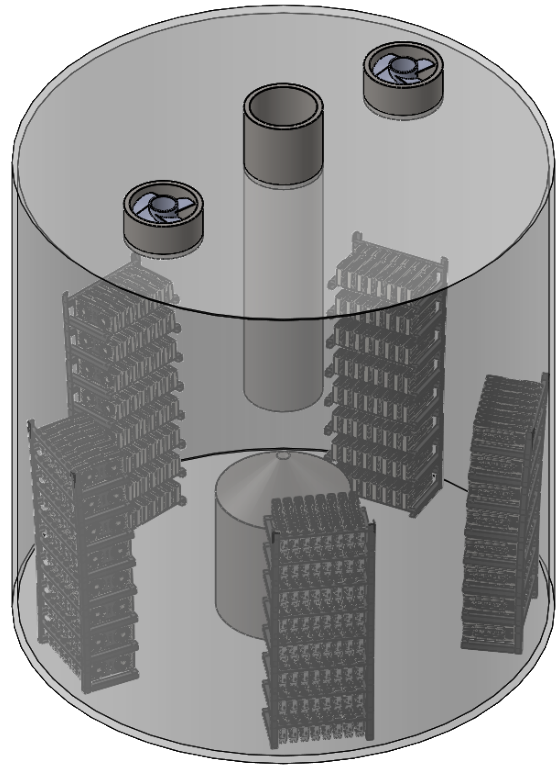

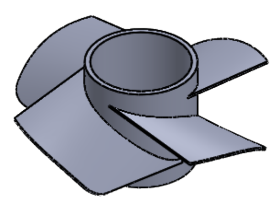

Extractor Fan

All Dimentions in Inches

PHONE
+1-403-5614723

EMAIL
info@aeroenergyc.com

WEB
www.aeroenergyc.com

APPENDIX B: Modified Concept Design of Vacuum Chamber

ALL DIMENSIONS IN INCHES

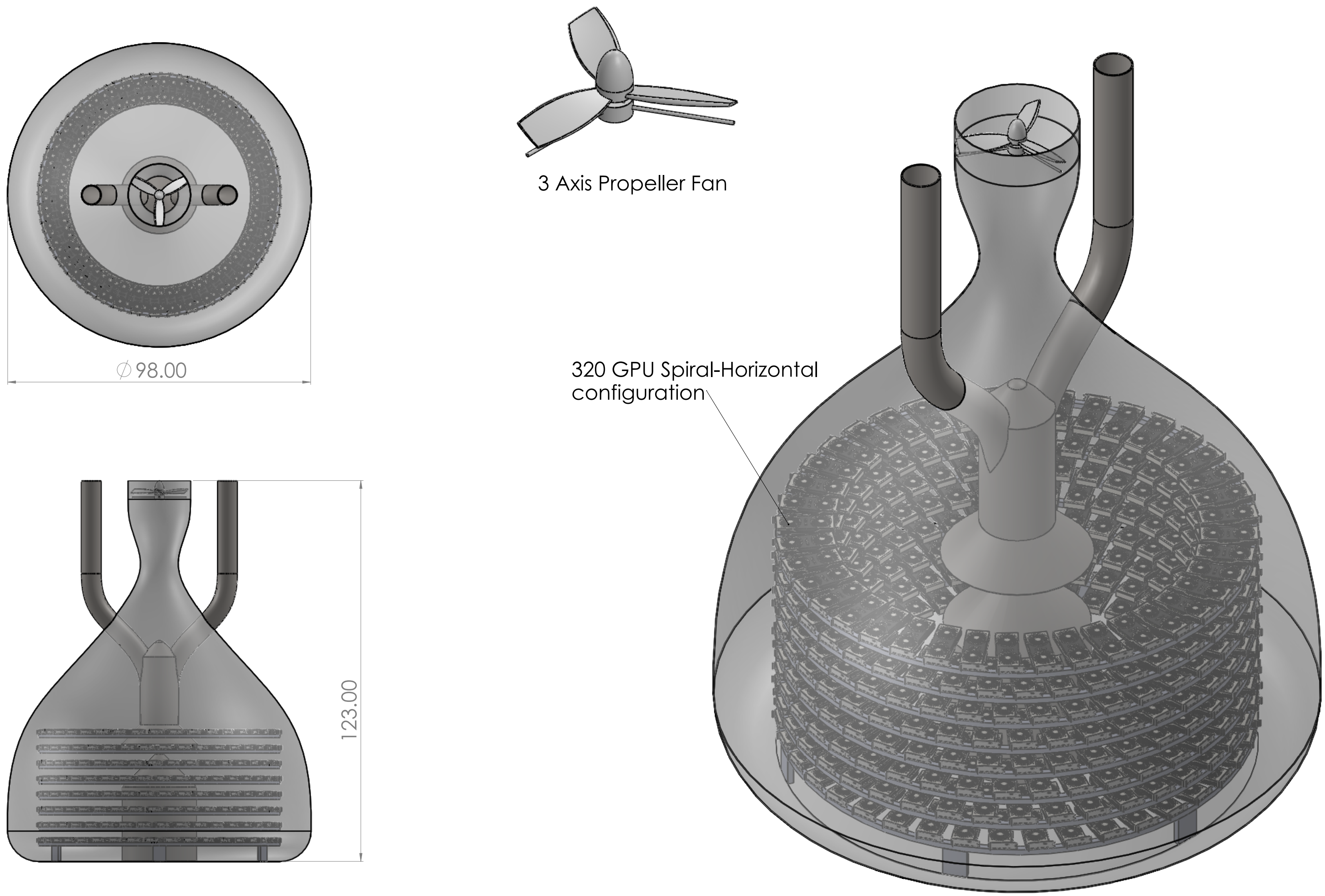

PHONE
+1-403-5614723

EMAIL
info@aeroenergyc.com

WEB
www.aeroenergyc.com

APPENDIX C: Modelled Concept Design of Vacuum Chamber

ALL DIMENSTIONS ARE IN INCHES

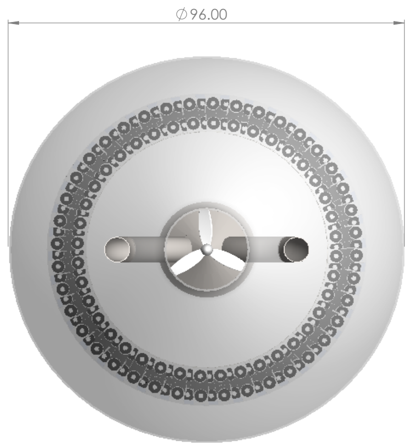

TOP VIEW

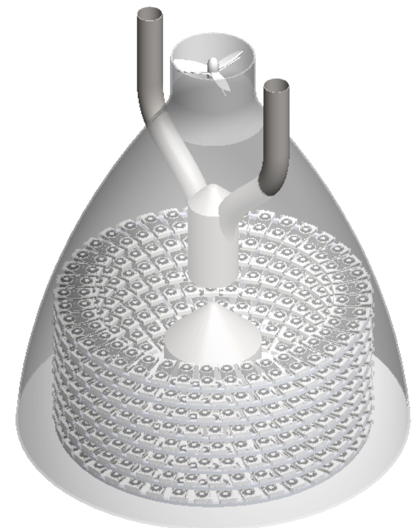

ISOMETRIC VIEW

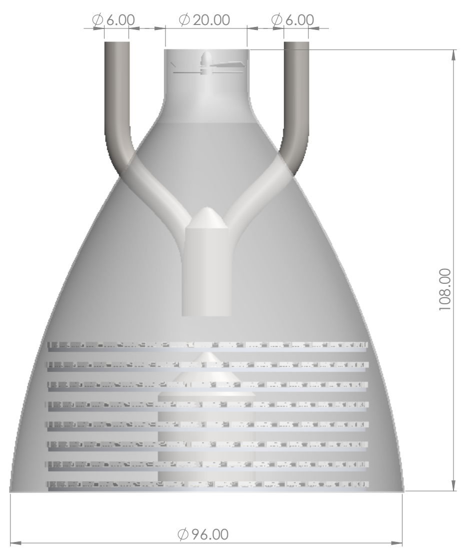

FRONT VIEW

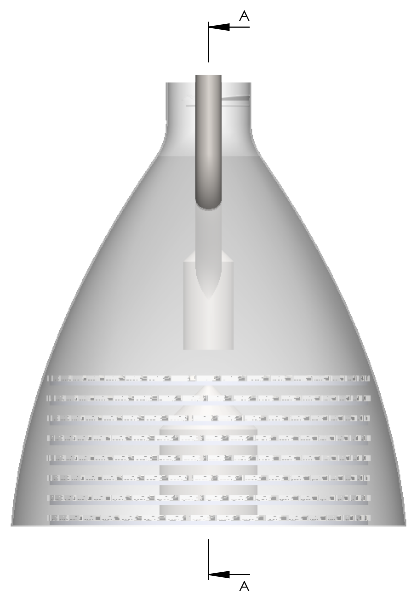

SIDE VIEW

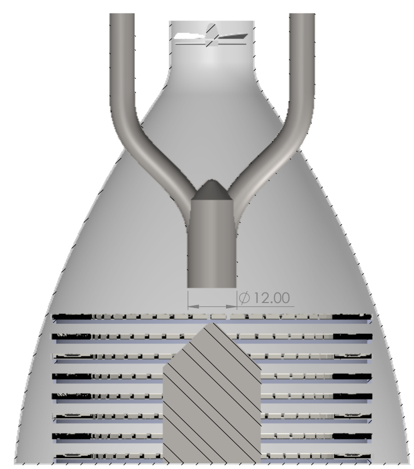

SECTION A-A
SCALE 1 : 20

PHONE
+1-403-5614723

EMAIL
info@aeroenergyc.com

WEB
www.aeroenergyc.com

APPENDIX D: Optimzed Concept Design of Vacuum Chamber

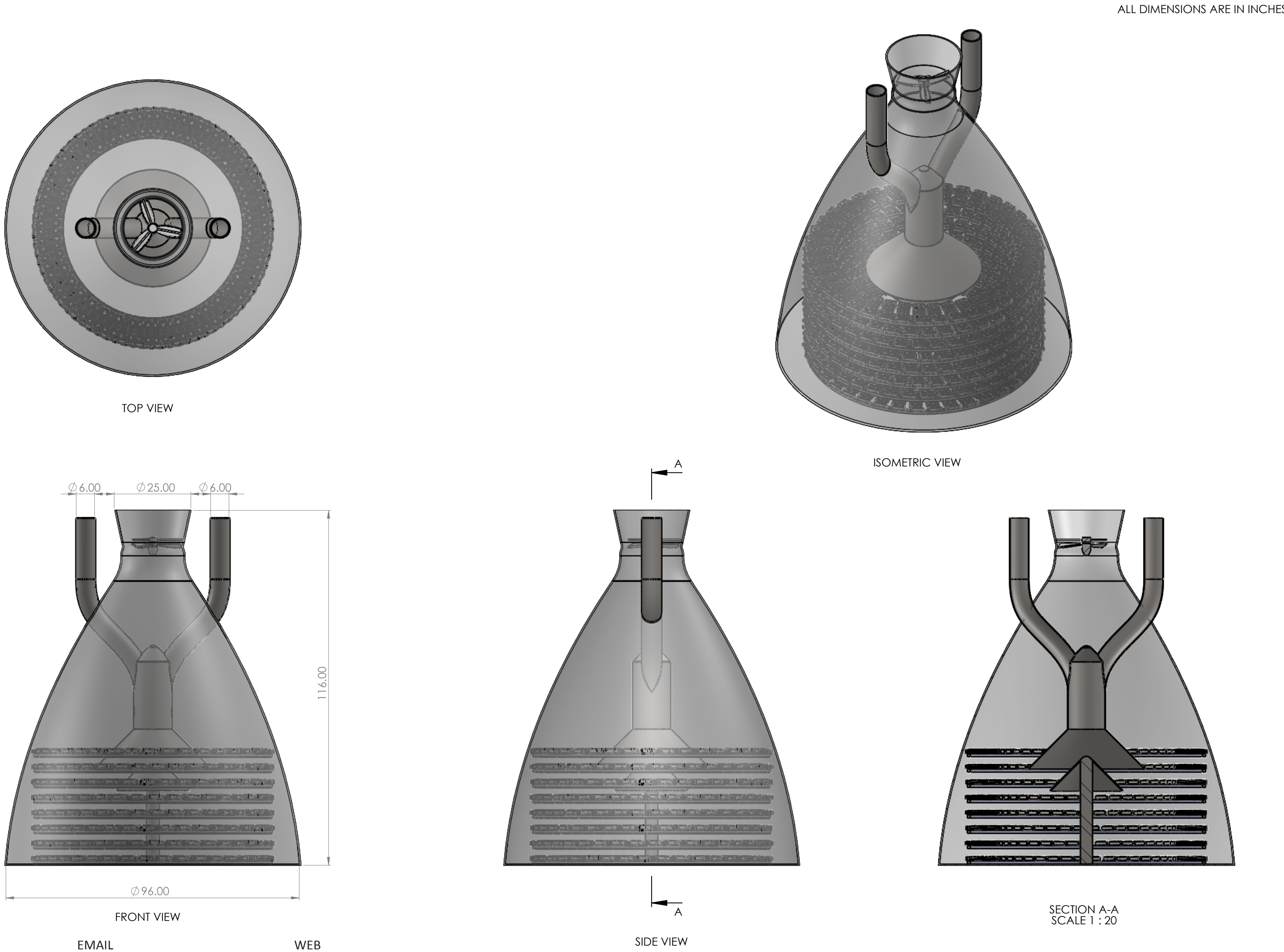

PHONE
+1-403-5614723

EMAIL
info@aeroenergyc.com

WEB
www.aeroenergyc.com